INTERNATIONAL JOURNAL OF CLIMATOLOGY, VOL. 10, 21–31 (1990) 551.513.7:551.524.36(4):551.526.6(261.2)

# EUROPEAN GROSSWETTER DURING THE WARM AND COLD EXTREMES OF THE EL NIÑO/SOUTHERN OSCILLATION

KLAUS FRAEDRICH
*Institut für Meteorologie, Freie Universität Berlin, D-1000 Berlin 41, FRG*

*Received 27 September 1988*
*Revised 2 December 1988*

## ABSTRACT

El Niño/Southern Oscillation (ENSO) warm and cold events affect the synoptic climatology of the north-eastern Atlantic–European sector. The classification of cyclonic and anticyclonic European Grosswetter (1881–1987) is analysed for its response on 26 warm and 21 cold ENSO episodes. Bi-monthly ranked composites computed over idealized 2-year ENSO warm (cold) episodes show more days of cyclonic (anticyclonic) steering over Europe. This signal is largest in the winter months of January and February following the year of a warm or cold event. The distributions of the occurrence of cyclonic and anticyclonic Grosswetter days are significantly different for warm and cold event winters: (i) there is more variability between individual warm event winter months, whereas the response to cold episodes is relatively uniform; (ii) on average, cyclonic Grosswetter days are experienced on 60 per cent (46 per cent) of the 58 warm (cold) event winter days—about 70 per cent (90 per cent) of the warm (cold) event winters realize more than 30 ($< 36$) days of cyclonic steering. Qualitatively corresponding results are obtained at a representative central European location for sunshine duration and the sum of daily negative temperatures, which characterize the winter strength.

KEY WORDS El Niño/Southern Oscillation European Grosswetter Mid-latitude response ENSO warm and cold events

## 1. INTRODUCTION

Observations and model results have shown that there are teleconnections between both phases of El Niño/Southern Oscillation (ENSO) events and the Northern Hemisphere (NH) extratropical circulation. In many observational studies the ENSO *warm event* response on regions adjacent to the forcing in the Pacific is analysed (e.g. Rasmussen and Carpenter, 1982; Ropelewski and Halpert, 1986). Some investigators include the observed extratropical teleconnections that are associated with ENSO *cold events* (e.g. van Loon and Rogers, 1981; Emery and Hamilton, 1985; Iwasaki and Hirota 1988). A large number of general circulation model (GCM) experiments (Shukla and Wallace, 1983; Geisler *et al.*, 1985; Mechoso *et al.*, 1987; and others) have simulated the response of the extratropical atmosphere to large positive sea-surface temperature (SST) anomalies (i.e. ENSO warm events), whereas only a few authors (e.g. Blackmon *et al.*, 1983; Palmer, 1985) have also considered teleconnections associated with negative SSTs (i.e. ENSO cold events) in GCMs.

Observational and GCM studies provide similar results for the North Atlantic–European sector; variations of the general circulation responses may be attributed to random effects, small changes in the boundary conditions of the forcings, and the structure of the large-scale non-linear dynamics (e.g. Geisler et al., 1985; Mechoso et al., 1987; Hamilton, 1988). Typical time-averaged patterns are the negative (positive) pressure or geopotential height anomalies during warm (cold) events with an equivalent barotropic response of the atmospheric mean fields over both the NH mid-latitude Pacific and Atlantic Oceans. Upper westerlies are intensified during warm events. Accordingly, the time resolution reveals enhanced baroclinic activity, which is associated with the warm events. Conjectured shifts of the North Atlantic storm tracks and observed changes in the meridional heat transport by standing eddies complete the picture of the response. However, much detail of statistical information on the synoptic climatology is lost if time-averaged fields of meteorological

0899–8418/90/010021–11$05.50

standard variables (like pressure, temperature, etc.) are analysed using episode-compositing or amplitude-correlation techniques.

This study analyses observations of ENSO warm and cold events affecting the distant large-scale circulation in the north-eastern Atlantic–European sector, which is described by the time series of the daily European Grosswetter classification in the form of a binary (cyclonic–anticyclonic) point process. The objective for this analysis is to make use of this uncommon data set in order to determine the response of the synoptic climatology over Europe to both ENSO warm and cold events. In Section 2 the data sets and the method of analysis are briefly outlined. In Section 3 we discuss the influence of warm and cold events in the tropical Pacific on various aspects of the European Grosswetter statistics (number of Grosswetter days, their period length, singularities, etc.) and on selected climate variables at a central European location (Berlin and Potsdam).

## 2. DATA AND METHOD OF ANALYSIS

### *2.1. European Grosswetter*

The data set analysed is the catalogue of 107 years of daily European Grosswetter (from 1881 to 1987). Every day is given one of 29 Grosswetter classes characterizing the sea-level pressure fields over Europe and the eastern North Atlantic (Hess and Brezowsky (1977), and issued routinely by the German Weather Service). They characterize the centres of action, their positions and steering, that dominate the area during a time span of a few days. These 29 large-scale weather classes are reduced to a set of two complementary circulation patterns, which form a dichotomous stochastic point process

$$G(t) = C \text{ or } A$$

with cyclonic ($C = 1$) or anticyclonic ($A = 0$) Grosswetter (steering) over Europe. The cyclonic state contains the Grosswetter class numbers 2, 3, 4, 6, 8, 11, 13, 15, 17, 19, 21, 23, 25, 27, 28 and 29 defined by Hess and Brezowsky (1977); the anticyclonic state is given by the remaining classes. This set has been used to identify intra-annual singularities of daily European weather dynamics and to evaluate their potential for long-range forecasting (see e.g. Baur, 1951; Gerstengarbe and Werner, 1987). In the following the bi-monthly number of days with cyclonic Grosswetter is analysed:

$$N(i,j) = \sum G(t) \quad \text{for} \quad t = T(i,j)$$

where $T(i,j)$ are the days in one of the six bi-months ($i = 1, \ldots, 6$) of the 107 years $j = 1881, \ldots, 1987$; for example, max $T(i = 1, j) = 58$ days. Bi-monthly values reduce the possible splitting of extended Grosswetter spells, which may last from the end of one month to the beginning of the next and retain the Grosswetter seasonality. Next, the number of bi-monthly cyclonic Grosswetter days ($=$max $T(i,j)$ minus the anticyclonic days) is ranked, $r = r(i,j) = 1, \ldots, 107$, for each bi-month $i$ from the smallest to the largest of the 107 years:

$$N(i,1) < \ldots < N(i,r) < \ldots < N(i,107)$$

The related percentile ranks $R(i,j) = 100r/107$ are then composited with respect to the El Niño/Southern Oscillation warm and cold events (following Meisner (1976); see also Ropelewski and Halpert (1986, 1987)) before the synoptic climatology of the European Grosswetter is analysed for the months of their largest response (Section 3).

### *2.2. ENSO warm and cold events*

These episodes cover an idealized 2-year period centred at the year of the event with half a year preceding and following it; ENSO peaks are observed at the end of the year of the event in December, January and February. The ENSO warm events included in this study are taken from Rasmussen and Carpenter (1983, table 2), plus the warm events of 1982 and 1986; this set has been used by Ropelewski and Halpert (1986, 1987). The warm event ensemble consists of 26 episodes (Table I, $j =$ warm) that are also covered by the Grosswetter data set.

Table I. Warm and cold extremes of the El Niño/Southern Oscillation (Rasmusson and Carpenter, 1983; van Loon and Shea, 1985)

| | | | | | | | | |
|---|---|---|---|---|---|---|---|---|
| Warm events ($j$=warm): | | | | | | | | |
| 1880 | 1884 | 1887 | 1891 | 1896 | 1899 | 1902 | 1905 | 1911 |
| 1914 | 1918 | 1923 | 1925 | 1930 | 1932 | 1939 | 1941 | 1951 |
| 1953 | 1957 | 1963 | 1965 | 1969 | 1972 | 1976 | 1982 | 1986 |
| Cold events ($j$=cold): | | | | | | | | |
| 1886 | 1889 | 1892 | 1898 | 1903 | 1906 | 1908 | | |
| 1916 | 1920 | 1924 | 1931 | 1938 | 1942 | 1949 | | |
| 1954 | 1964 | 1966 | 1970 | 1973 | 1975 | 1978 | | |

The ensemble of 21 years of cold events (Table I, $j$ = cold) are those given by van Loon and Shea (1985, table 1) plus the year 1975 (van Loon, pers. comm.). The binary Grosswetter point process of daily synoptic classification is composited about the ENSO warm and cold events to provide details of time statistics that remain unresolved by the more common correlation analyses of mean fields.

## 3. RESULTS

### 3.1. *Response to ENSO warm and cold events*

The cyclonic European Grosswetter statistic (i.e. the average percentile rank of the bi-monthly number of days with a cyclonic state of the large-scale circulation) is estimated and composited for the years of ENSO warm and cold events separately, with half a year preceding and following:

$$\langle R(i,j)\rangle \quad \text{from} \quad (i=4; j-1) \quad \text{to} \quad (i=3; j+1) \quad \text{for} \quad j=\text{warm or cold}$$

These ensemble averages, $\langle\ \rangle$, are shown in Figure 1, centred at the 50 per cent level to visualize the deviations from the long-term mean. Note that for the total time series of $J = 107$ years, the mean and variance of the percentile ranks, $R(i,j)$, are $\langle R(i,j)\rangle = 0{\cdot}5 + 0{\cdot}5/J$ and $(1 - 1/J^2)/12$; for large $J$ the average ($\pm$standard deviation) tends to 50 per cent ($\pm 28{\cdot}9$ per cent).

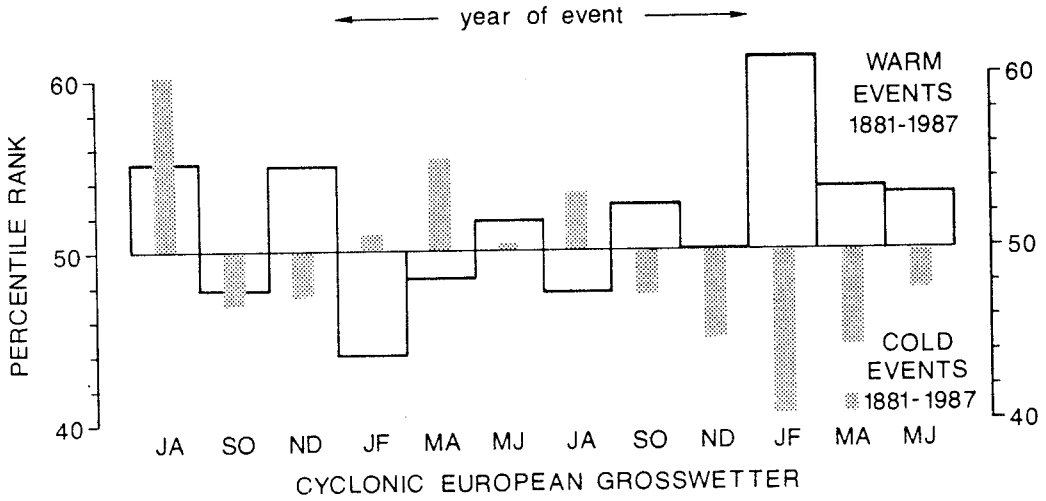


Figure 1. Percentile ranks of the number of cyclonic European Grosswetter days composited about El Niño/Southern Oscillation warm and cold events. The bi-monthly percentile rank values represent an average over 25 warm (open columns) and 21 cold events (stippled columns). The composite includes half a year preceeding and following the year of the event

The differences between warm and cold events appear to be negligible in the year of the event and the 6 months preceding it. The largest response is observed in the NH winter at the peak of the event. In particular the winter bi-month January/February shows large and opposing deviations from the mean: a reduced number of cyclonic Grosswetter days for cold events, an enhanced number for warm events, and vice versa for the anticyclonic steering. Both cold and warm event signals (i.e. the maximum percentile rank deviations from the 50 per cent mean) decay gradually in spring. But only the cold event deviation starts growing in the autumn of the year of the event, whereas the warm event response commences abruptly in January/February. The difference between the warm and cold event winter signals is largest for the bi-month January/February. Using the distribution-free Wilcoxon (or Mann-Whitney) two-sided rank sum test one can reject the null-hypothesis with 95 per cent confidence that both the warm and cold Grosswetter occurrences have the same statistical population in common. Therefore, we confine the following discussion of ENSO warm and cold events affecting the European Grosswetter to these winter months.

### *3.2. Winter singularities*

For every calendar day the relative frequency of cyclonic Grosswetter occurrence (= 100 per cent minus the anticyclonic frequency) can be determined by the ensemble average, $\langle\ \rangle$, over the $j$ = warm or $j$ = cold events:

$$\langle G(t)\rangle$$

where $t = T(i = 1, j + 1)$ are the days of January and February following the year of the event. The first 15 waves of the harmonically analysed ensemble averages (from December to March) are presented in Figure 2 for warm and cold events, to add more details to the bi-monthly rank statistic; they describe about 80 per cent of the variance, with contributions by periods of a week and longer to determine the extended spells of Grosswetter singularities. The warm event frequency of cyclonic Grosswetter exceeds that of the cold events on almost every day in January and February. Averaged over the two months, cold events tend to generate less cyclonic than anticyclonic steering over Europe. The related probability of occurrence of cyclonic Grosswetter

$$p = \langle N(i = 1, j + 1)\rangle/58$$

is estimated: $p$(warm) = 60 per cent for the warm and $p$(cold) = 46 per cent for the cold event ensemble (53 per

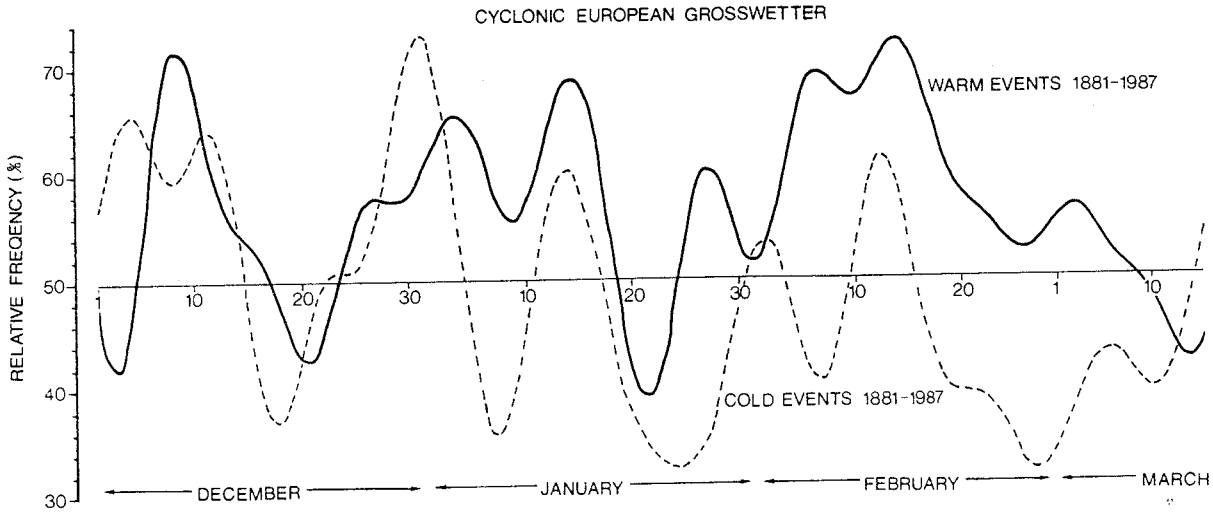


Figure 2. Calendar singularities: daily cold and warm event relative frequency of cyclonic (= 100 per cent minus anticyclonic) Grosswetter occurrence in Europe

cent for the total). The associated 90 per cent confidence limits for the $J = 26$ warm ($J = 21$ cold) events yield

$$\pm 1{\cdot}282[p(1-p)/J]^{1/2} = \pm 0{\cdot}12 \quad \text{for warm}$$
$$= \pm 0{\cdot}13 \quad \text{for cold events}$$

That is, the average cyclonic (and also anticyclonic) Grosswetter occurrence is different for warm and cold winter episodes at the 90 per cent significance level. Furthermore, one can expect cyclonic Grosswetter on every day in January and February with a probability of $p$(warm) = 60 per cent, $p$(cold) = 46 per cent. Now, a calendar singularity can be defined, if a particular day, $t = t^*$, in the bi-monthly period exceeds the 90 per cent confidence intervals of the two probability estimates, which are assumed to hold for every day of January and February (see also Bissolli and Schönwiese (1987)). That is, a singularity of cyclonic or anticyclonic Grosswetter can be expected (with 90 per cent significance) if its relative frequency in the warm (cold) event ensemble exceeds the following limits on that day: $\langle G(t = t^*)\rangle > 72$ per cent or $< 48$ per cent ($> 60$ per cent or $< 34$ per cent).

Thus, cyclonic (or anticyclonic) singularities can be expected in mid-February (or near 20 January) when cyclonic steering over Europe has occurred in more than 18 (or less than 11) of the 26 warm episodes. For cold events, cyclonic singularities can only be realized near the end of the year, around 31 December; anticyclonic singularities have been observed at about 24 January and at the end of February. It appears that instabilities in the dates of the European weather singularities, if their significance is sufficiently large, may be linked to the changing occurrence of ENSO warm and cold events. That is, a singularity observed in one climate epoch can vanish in another because the occurrence of ENSO events may have changed. Recent studies casting doubt on the stability of singularities in different climate epochs (Gerstengarbe and Werner, 1987) seem to support this; but ENSO may not be the only cause of the instability of calendar singularities.

### *3.3. Distributions of Grosswetter*

Considering the cyclonic–anticyclonic European Grosswetter, $G(t)$, as a binary stochastic point process, various associated statistical distributions can be deduced (not unlike the energetics that are associated with a dynamical process) to gain more insight into the synoptic climatology.

#### *3.3.1. Occurrence*

The distribution (density) of the bi-monthly number of cyclonic (anticyclonic) Grosswetter days occurring in January/February

$$P(N) = \text{prob}[N(i = 1, j + 1) \quad \text{for } j = \text{warm or cold}]$$

is estimated and presented in Figure 3 as a frequency distribution for all warm and cold events, and for all years. The following differences between the warm and cold event distributions are noteworthy. (i) On average, the $j$ = warm events generate more cyclonic Grosswetter days than cold events, with the ensemble mean $\langle N(i = 1, j + 1)\rangle$ plus/minus standard deviation of $35 \pm 16$ days (i.e. $p = 60$ per cent). Note also that the number of cyclonic Grosswetter days is so low ($p = 46$ per cent) in $j$ = cold event winters ($27 \pm 17$) that, on average, more anticyclonic days are realized. The total average lies in between, with $31 \pm 22$ days in the cyclonic state (see Section 3.2 for confidence limits). (ii) The warm or cold event distributions are shifted accordingly to the upper or lower side of the spectrum. From a chi-squared goodness-of-fit test we can conclude that both distributions originate from different populations at a 95 per cent level of significance. (iii) More specifically, 19 out of 21 (90 per cent) cold event winters have shown less than 36 (of the 58 possible) cyclonic Grosswetter days in the bi-month period; conversely, 19 out of 26 (73 per cent) warm event winters have realized more than 30 (of the 58 possible) cyclonic Grosswetter days in January and February. (iv) Finally, the warm events tend to generate winters in Europe that vary more from episode to episode, but the cold event winters appear to be more uniform (see also Emery and Hamilton (1985)). The modal value (or about half of the cold event winters) falls into the class of 30–35 days of cyclonic steering.

The difference between the warm and cold event distributions may be due either to a significant change of the dynamical structure of the atmosphere or it may merely reflect a shift of the boundary conditions with

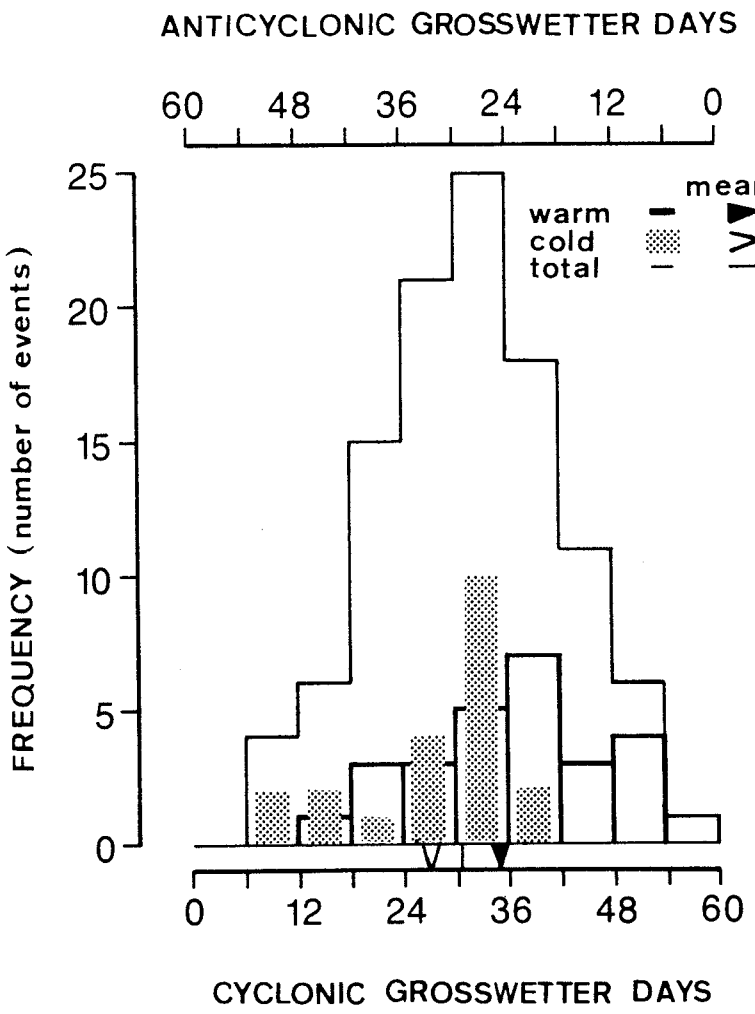


Figure 3. Frequency distributions of the number of cyclonic (anticyclonic) European Grosswetter days in January and February for 26 warm event, 21 cold events, and the total of 107 years. Averages are indicated at the bottom line

conservation of the underlying dynamics. Some insight into the cause of this difference can be gained from the following time distributions.

*3.3.2. Residence time (period length)*

The duration of a Grosswetter spell is the period length or residence time of the binary Grosswetter process in its cyclonic or anticyclonic state, $L(C)$ or $L(A)$:

$$P[L(C)=n]=\text{prob}\{G[t+(n+1)]=A \text{ with } G(t+n)=G[t+(n-1)]\ldots=C \text{ and } G(t)=A\}$$

where $n$ counts the number of days with $t+n=T(i=1,j+1)$ for $j=$ warm or cold. The relative frequency distribution of the duration of cyclonic Grosswetter spells is presented in Figure 4. There are fewer short spells (with period lengths $<4$ days) and more long spells (between 9 and 12 days) of cyclonic Grosswetter observed for warm events than for cold events, which corresponds with the reduced number of cold event cyclonic days. However, the observed differences of the period-length distributions are not large enough to conclude that they are generated by different populations (i.e. the differences between warm and cold event period lengths, etc. are statistically not significant). Therefore, we can assume from this data set that the processes governing

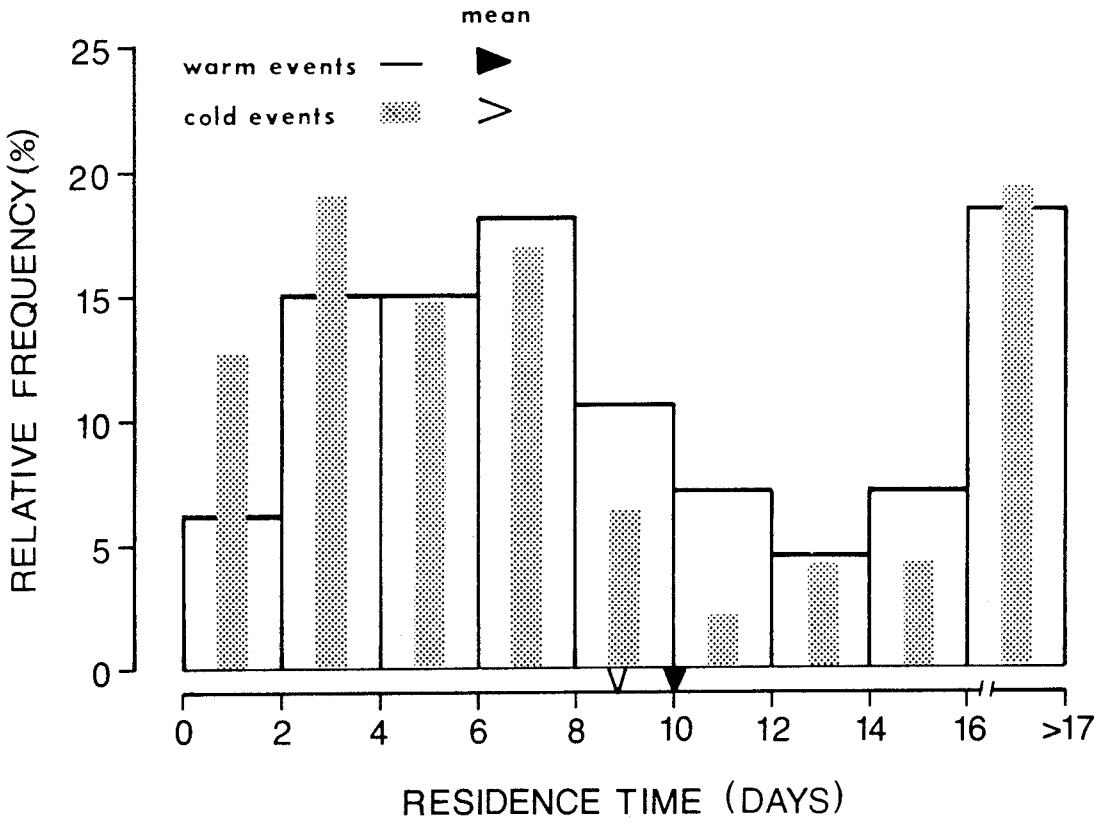


Figure 4. Relative frequency of the duration of spells (period length or residence time) of cyclonic Grosswetter for warm and cold events in January and February for 26 warm and 21 cold events. Averages are indicated at the bottom line; note the scale change for the last column (>17 days)

the dynamics of the European Grosswetter response cannot be distinguished for both ENSO warm and cold events (even at a 85 per cent significance level); that is, we are seeing differences in the boundary conditions.

*3.3.3. First passage time*

The same can be concluded from the differences between warm and cold event distributions of the first passage time, $F(A, C)$. This time elapses between state $A$ (= anticyclonic), say, and state $C$ (= cyclonic), which has been avoided at times $t < t+v < t+m-1$.

$$P[F(A, C)=m] = \text{prob}[G(t+m)=A \text{ with } G(t+v)=C \quad \text{for } 1<v<m-1 \text{ and } G(t)=C]$$

where $m$ counts the number of days with $t+m=T(i=1, j+1)$ for $j=$ warm or cold. In this sense $F(A, C)$ is a measure of change from the anticyclonic to the cyclonic Grosswetter state.

This statistic bears similarity with variance analyses in the time domain, if the number of first passages is weighted by the first passage time ($F\,P(F)$). The related distributions (Table II) show the relative amount that a given first passage time from the anticyclonic to the cyclonic state contributes to the total time of all such passages. Noteworthy, in a qualitative sense, is that the maximum contribution changes from the 9–10-day first passage time in cold events to the 5–6-day class for warm events. This indicates enhanced activity (i.e. changes from the anticyclonic state to the cyclonic one) of shorter time-scales in warm event winters and vice versa. It is the difference in the 9–10-day class that makes the time-weighted statistics of warm and cold events (Table II) significantly different from one another (at the 99 per cent level). The complementary passage (from $C$ to $A$) does not reveal the same signal. (For definitions of first passage time and period length see, e.g., Fraedrich (1988)).

Table II. Relative contribution (per cent) of first passage times (in days) to the total time spent in the transition from anticyclonic to cyclonic Grosswetter (3400 days for warm and 2739 days for cold events)

| | First passage time | | | | | | | | |
|---|---|---|---|---|---|---|---|---|---|
| | 1–2 | 3–4 | 5–6 | 7–8 | 9–10 | 11–12 | 13–14 | 15–16 | >17 days |
| Warm events | 6·6 | 11·4 | *13·0* | 11·8 | 10·0 | 8·4 | 7·9 | 4·1 | 26·8 |
| Cold events | 5·8 | 10·6 | 12·0 | 13·1 | *13·4* | 9·2 | 7·4 | 4·5 | 24·0 |

### *3.4. Related general circulation model (GCM) simulations*

As suggested in the introduction, some of the empirical results can be recognized in recent GCM experiments studying the atmospheric response in NH winter to temperature anomalies over the equatorial Pacific (Palmer, 1985, fig. 5; Mechoso *et al.*, 1987, figs. 13b and 16b).

(i) In the NH mid-latitudes the winter mean 700 mbar or 200 mbar geopotential height fields show a distinct negative (positive) anomaly over Europe, which, at least qualitatively, corresponds to the larger (smaller) number of days of cyclonic European Grosswetter observed in warm (cold) event winters.

(ii) In the model experiments of warm event winters the upper tropospheric mid-latitude westerlies are intensified, which, in turn, generate more active synoptic-scale transient baroclinic waves in a zonal belt extending from the north-eastern Pacific to the northern Atlantic. This is supported by the observed larger variability of the number of cyclonic (or anticyclonic) Grosswetter days in warm event European winters.

(iii) Model and observed wavenumber-frequency spectra change the maximum variance contributions from the eastward travelling wavenumber 4, with a period of about 10 days, to the wavenumber 6, with a period of about 4 days, during ENSO warm event winters (Fraedrich and Böttger, 1978; Mechoso *et al.*, 1987). In a qualitative sense this does not contradict the observation that in warm (cold) event winters, short (longer) first passage times from the anticyclonic to the cyclonic Grosswetter state of 5–6 days (9–10 days) contribute most to the total time spent in transition. The first passage from the cyclonic to the anticyclonic state does not exhibit such a clear distinction. But note, however, that a statistic of the first passage time does not allow direct conclusions on the variance contributions of the processes involved.

### *3.5. Warm and cold event winters at a central European station (Berlin and Potsdam)*

In order to relate the synoptic climatology over Europe with the climate at a particular site, we analyse two weather variables characterizing the strength of the winter months of January/February at a central European location (Berlin and Potsdam): the sunshine duration and the sum of the negative daily mean temperatures (Figures 5 and 6). As the precipitation amount did not reveal a notable ENSO response in central Europe (see also Ropelowski and Halpert (1987)), these results are not presented.

(i) The distributions of the sunshine duration (relative to the maximum possible of 532·3 h), or its complement, the cloudiness, are analysed for 22 warm and 19 cold events, and all the 94 winters that were available for Potsdam (near Berlin). In central Europe we observe (Figure 5) an average $23{\cdot}2 \pm 6{\cdot}4$ per cent of the astronomically possible sunshine, with less during warm event winters ($21{\cdot}7 \pm 8{\cdot}2$ per cent) than for cold events ($23{\cdot}7 \pm 5{\cdot}4$ per cent). Despite the relatively small distance between warm and cold event averages the distributions show larger differences: only 36 per cent (8 of 22) of the warm event winters, but as much as 74 per cent (4 of 19) of the cold event winters realize more than the average amount of sunshine. Maximum frequencies of warm events are found in either one of the low sunshine classes between 10 per cent and 21 per cent, but for cold events they occur in the higher class of 22–27 per cent. Again, the distribution of warm event winters covers a wider range of sunshine durations (associated with a larger standard deviation) than the cold event distribution. The difference between both is significant at the 85 per cent level using the chi-squared test.

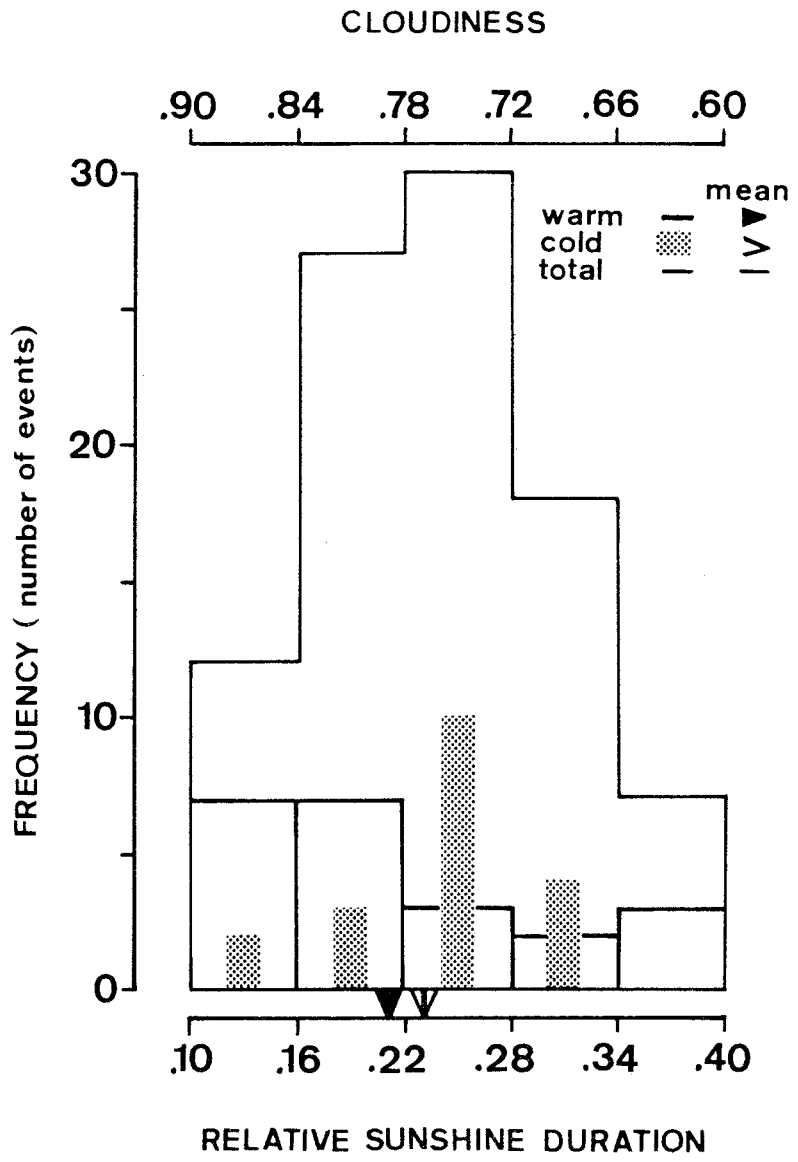


Figure 5. Frequency distributions of the relative sunshine duration (or its complement, the cloudiness) at Potsdam in January and February for 22 warm events, 19 cold events, and a total of 94 years. The averages are indicated at the bottom line

This relatively low significance level is not surprising because the sunshine duration is a variable linked with both meso- and synoptic-scale dynamics.

(ii) The sum of the negative daily mean temperatures is another suitable measure of the strength of a winter. For a central European station (Berlin) the analysis of a complete record of 107 years (Figure 6) shows that warm event winters tend to be more severe ($134 \pm 91$°C) than the cold event ones ($97 \pm 73$°C). The distributions show similar features as those of the relative sunshine duration but they are less pronounced. For 14 out of 27 (52 per cent) warm event winters the daily negative temperatures contribute more than (negative) 120°C (not far from the total average of $110 \pm 80$°C). But only 5 out of 21 (24 per cent) cold event winters fall into this category. Qualitatively, the warm events appear to generate severe, average, and mild winters with almost equal probabilities, but cold event winters are more frequently on the milder side of the spectrum. However, it should be noted that the statistical significance of the warm–cold event difference of the

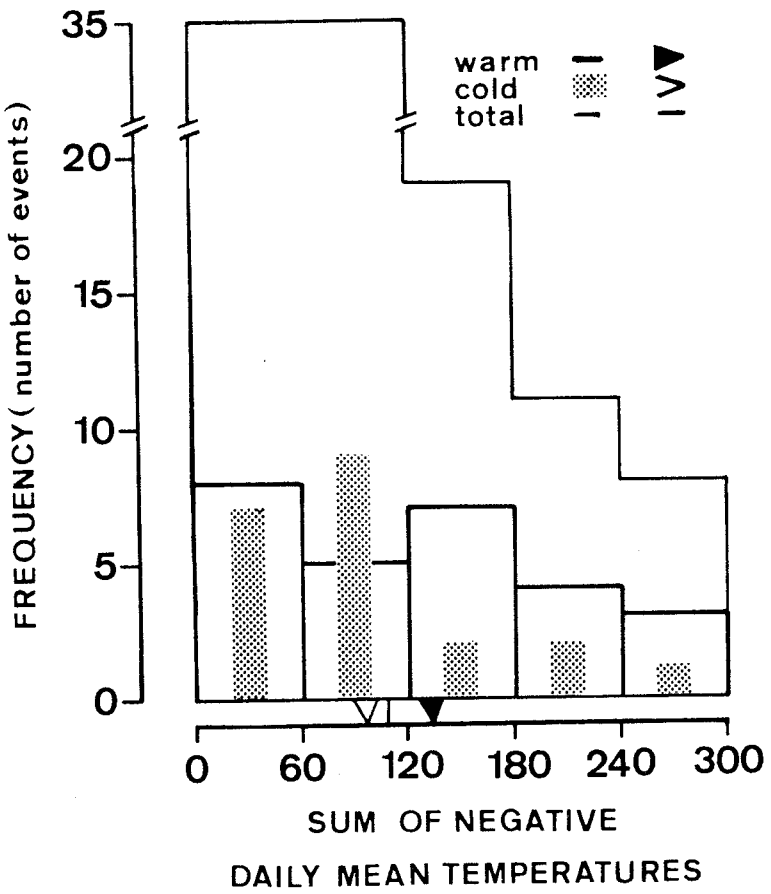


Figure 6. Frequency distribution of the sum of negative daily mean temperatures at Berlin in January and February for 26 warm events, 21 cold events, and the total of 107 years. The averages are indicated at the bottom line

distribution of this variable is below that of the sunshine duration. Furthermore, the null hypothesis that the warm and cold event averages belong to populations of the same mean also cannot be rejected (applying the two-sided $t$-test with 45 degrees of freedom and assuming a 95 per cent level of significance).

## 4. SUMMARY AND DISCUSSION

The synoptic climatology over Europe and some climate variables at a central European location have been related to warm and cold events of the El Niño/Southern Oscillation. The objective of this study was the analysis of an uncommon data set: a 107-year (and routinely updated) record of European Grosswetter, which emphazises the day to day synoptic aspects of the large-scale circulation in the European–North Atlantic sector in terms of a binary (cyclonic–anticyclonic) classification. First, a composite rank statistic describes qualitatively the difference between warm and cold ENSO forcing of the synoptic situation over Europe, and that of its timing. Not unexpectedly, the largest response is observed in the NH winters following the year of the event, in particular in January and February. While the cold event response tends to follow a life cycle of growth (in autumn) and decay (in spring), with a peak at the core of the winter, the warm event signal appears to reach its peak almost abruptly before it gradually decays. A comparison between the warm and cold event distributions adds quantitative statistical information. It turns out that the occurrence of cyclonic (anticyclonic) European Grosswetter (Figure 3), the relative sunshine duration (cloudiness, Figure 5) at Potsdam, and the sum of negative daily temperatures at Berlin (Figure 6) are related in their response to ENSO warm and cold events.

(i) Warm events are associated with highly variable winters; that is, there are large differences observed in the high winter season (January and February) of one episode to another one. Cold events, however, appear to produce a more uniform response with less variation between the individual events and, therefore, may have a higher predictability in long-range forecasting.

(ii) Warm episodes tend to produce more cyclonic and less anticyclonic Grosswetter situations over Europe than their cold counterparts. Correspondingly, the cold event winters tend to have more sunshine in central Europe and appear to be less severe, on average, than those of the warm events, irrespective of their inherent larger variability.

Finally it should be noted that the 1988 ENSO cold event was associated with the following January/February 1989 Grosswetter situation in Europe, which supports the above results: 19 cyclonic Grosswetter days (with anticyclonic steering during the expected calendar singularity about the 24th of January, but cyclonic steering at the end of February), 29 per cent relative sunshine duration in Potsdam, and 2·5°C as the sum of negative daily mean temperatures in Berlin.

ACKNOWLEDGEMENT

Discussions with Dr K. Müller, A. Tornow and R. Kuglin, computations by K. Müller and H. Haug, and drawing by Ms Ch. Kirsch and H. Haug are appreciated.

REFERENCES

Baur, F. 1951. 'Extended-range weather forecasting', in Malone, T. F. (ed.) *Compendium of Meteorology*, American Meteorological Society, Boston, pp. 811–833.

Bissolli, P. and Schönwiese, C. D. 1987. 'Singularitäten in der Bundesrepublik Deutschland 1946–1986. Vorläufige Ergebnisse einer statistischen Analyse anhand ausgewählter Stationen', *Meteorol. Rundsch.*, **40,** 147–155.

Blackmon, M. L., Geisler, J. E. and Pitcher, E. J. 1983. 'A general circulation model study of January climate anomaly patterns associated with interannual variation of equatorial Pacific sea surface temperatures', *J. Atmos. Sci.*, **40,** 1410–1425.

Emery, W. J. and Hamilton, K. 1985. 'Atmospheric forcing of interannual variability in the northeast Pacific Ocean: connections with El Niño', *J. Geophys. Res.*, **90,** 857–868.

Fraedrich, K. 1988. 'El Niño/Southern Oscillation predictability', *Mon. Wea. Rev.*, **116,** 1001–1012.

Fraedrich, K. and Böttger, H. 1978. 'A wavenumber-frequency analysis of the 500 mb geopotential at 50°N', *J. Atmos. Sci.*, **35,** 745–750.

Geisler, J. E., Blackmon, M. L., Bates, M. L. and Munoz, S. 1985. 'Sensitivity of January climate response to magnitude and position of warm equatorial Pacific sea surface temperature anomaly', *J. Atmos. Sci.*, **42,** 1037–1049.

Gerstengarbe, F.-W. and Werner, P. C. 1987. 'Ist der Baur'sche Kalender der Witterungsregelfälle heute noch gültig?', *Z. Meteorol.*, **37,** 263–272.

Hamilton, K. 1988. 'A detailed examination of the extratropical response to tropical El Niño/Southern Oscillation events', *J. Climatol.*, **8,** 67–86.

Hess, P. and Brezowsky, H. 1977. *Katalog der Grosswetterlagen*, Ber. Dtsch. Wetterdienst, Offenbach, 113, Bd. 15, 39 pp.

Iwasaki, T. and Hirota, I. 1988. 'The influence of the Southern Oscillation on extratropical circulations during the Northern Hemisphere winter', *J. Meteorol. Soc. Jpn*, **66,** 419–432.

Mechoso, C. R., Kitoh, A., Moorthi, S. and Arakawa, A. 1987. 'Numerical simulations of the atmospheric response to a sea surface temperature anomaly over the equatorial eastern Pacific Ocean', *Mon. Wea. Rev.*, **115,** 2936–2956.

Meisner, B. N. 1976. *A Study of Hawaiian and Line Island Rainfall*, Department of Meteorology, University of Hawaii, Honolulu, Rep. UHMET 76-4, 82 pp.

Palmer, T. N. 1985. 'Response of the UK Meteorological Office General Circulation Model to sea-surface temperature anomalies in the tropical Pacific Ocean', in Nihoul, C. J. (ed.) *Coupled Ocean–Atmosphere Models*, Elsevier, Amsterdam, pp. 83–107.

Rasmusson, E. M. and Carpenter, T. H. 1982. 'Variations in tropical sea surface temperature and surface wind fields associated with the Southern Oscillation/El Niño', *Mon. Wea. Rev.*, **110,** 354–384.

Rasmusson, E. M. and Carpenter, T. H. 1983. 'The relationship between eastern equatorial Pacific sea surface temperatures and rainfall over India and Sri Lanka', *Mon. Wea. Rev.*, **111,** 517–528.

Ropelewski, C. F. and Halpert, M. S. 1986. North American precipitation and temperature patterns associated with the El Niño/Southern Oscillation (ENSO)', *Mon. Wea. Rev.*, **114,** 2352–2362.

Ropelewski, C. F. and Halpert, M. S. 1987. 'Global and regional scale precipitation patterns associated with the El Niño/Southern Oscillation', *Mon. Wea. Rev.*, **115,** 1606–1626.

Shukla, J. and Wallace, J. M. 1983. 'Numerical simulation of the atmospheric response to equatorial Pacific sea surface temperature anomalies', *J. Atmos. Sci.*, **40,** 1613–1630.

Van Loon, H. and Madden, R. A., 1981. 'The Southern Oscillation. Part I. Global associations with pressure and temperature in northern winter', *Mon. Wea. Rev.*, **109,** 1150–1162.

Van Loon, H. and Rogers, J. C. 1981. 'The Southern Oscillation. Part II. Associations with changes in the middle troposphere in the northern winter', *Mon. Wea. Rev.*, **109,** 1163–1168.

Van Loon, H. and Shea, D. J. 1985. 'The Southern Oscillation. Part IV. The precursors south of 15°S to the extremes of the oscillation', *Mon. Wea. Rev.*, **113,** 2063–2074.